Advances in Concrete Construction, *Vol. 9, No. 4 (2020) 387-395*
DOI: https://doi.org/10.12989/acc.2020.9.4.387

Development of fiber reinforced self-compacting concrete (FRSCC): Towards an efficient utilization of quaternary composite binders and fibers

Roman Fediuk[1a], Mohammad A. Mosaberpanah*[2] and Valery Lesovik[3a]

[1]*School of Engineering, Far Eastern Federal University, Vladivostok, Russian Federation*
[2]*Department of Civil Engineering, Cyprus International University (CIU), Nicosia, North Cyprus, Turkey*
[3]*Building Materials Science, Products and Structures, Belgorod State Technological University, Belgorod, Russian Federation*

(*Received December 17, 2019, Revised February 17, 2020, Accepted March 6, 2020*)

Abstract. This study has been carried out in two-phases to develop Fiber Reinforced Self-Compacting Concrete (FRSCC) performance. In the first phase, the composition of the quaternary composite binder compromised CEM I 42.5N (58-70%), Rice Husk Ash (25-37%), quartz sand (2.5-7.5%) and limestone crushing waste (2.5-7.5%) were optimized. And in the second phase, the effect of two fiber types (steel brass-plated and basalt) was investigated on the SCC optimized with the optimum CB as disperse reinforcement at 6 different ratios of 1, 1.2, 1.4, 1.6, 1.8, and 2.0% by weight of mix for each type. In this study, the theoretical principles of the synthesis of self-compacting dispersion-reinforced concrete have been developed which consists of optimizing structure-formation processes through the use of a mineral modifier, together with ground crushed cement in a vario-planetary mill to a specific surface area of 550 m2 / kg. The amorphous silica in the modifier composition intensifies the binding of calcium hydroxide formed during the hydration of C3S, helps reduce the basicity of the cement-composite, while reducing the growth of portlandite crystals. Limestone particles contribute to the formation of calcium hydrocarbonate and, together with fine ground quartz sand; act as microfiller, clogging the pores of the cement. Furthermore, the results revealed that the effect of fiber addition improves the mechanical properties of FRSCC. It was found that the steel fiber performed better than basalt fiber on tensile strength and modulus of elasticity; however, both fibers have the same performance on the first crack strength and sample destruction of FRSCC. It also illustrates that there will be an optimum percentage of fiber addition.

Keywords: FRSCC; quaternary composite binders; fibers; mechanical properties; first crack; destruction

1. Introduction

Effective concretes for protective structures in connection with the increasing number of natural (including global climate change) and man-made (including increased international tensions and terrorist acts) disasters are now of particular importance. For these concretes, the special set of characteristics are needed to amend static compressive, tensile strength, impact strength (dynamic strength), crack resistance, impermeability and workability (Chen *et al.* 2018, Djelloul *et al*. 2018, Fediuk *et al*. 2018, Mosaberpanah and Eren 2017b). The design of materials that can provide a complex of these characteristics at a given level is possible only with the use of the latest advances in building materials science and in the management of structure formation processes through the use of multicomponent systems (Danish and Mosaberpanah 2020, Mosaberpanah and Eren 2016). At the same time, concern for human life and health from the standpoint of the "man-material-environment" system should be taken into account even at the material production stage. Reducing the consumption of clinker raw materials and the energy intensity of manufacturing materials, as well as the recycling of industrial waste are essential steps toward sustainable development (Khaloo *et al*. 2014, Mosaberpanah and Eren 2018, Svintsov and Shambina 2018, Vincler *et al.* 2019).

Self-compacting concrete (SCC) is a composite material with high flow capacity which could spread through congested reinforcement by its own weight. Thus, it seems expedient to develop self-compacting concretes with a view to increase their efficiency through the use of promising composite binders using local raw materials and industrial waste (Abdelgader *et al*. 2010, AlTaan *et al*. 2012, Yu *et al*. 2018).

The development of various protective concretes (radiation-protective, heat-resistant, impact-resistant, impermeable, bioprotective, etc.) has been studied in sufficient detail earlier (AlTaan *et al*. 2012, Dauji and Bhargava 2016, Suleymanova *et al*. 2014, Volodchenko *et al.* 2015). As a result of the theoretical analysis, it was established that natural (earthquakes, hurricanes, extreme temperatures, forest fires, water, snow, ice, etc.) and man-made (shock wave, radiation, toxic substances, sound and others) damaging factors have enormous impact on civil protective structures (Zagorodnjuk *et al.* 2016). In this regard, the actual scientific and technical challenge is to develop a new generation composites, which are characterized by a special set of required high performance: static and impact strength in compression, tensile strength,

*Corresponding author, Assistant Professor
E-mail: mmosaberpanah@ciu.edu.tr
[a]Professor

ISSN: 2287-5301 (Print), 2287-531X (Online)

elastic modulus, vapor- and gas- impermeability, workability. It was proved that the creation of high-density and high-strength composites is possible by controlling the processes of structure formation of multicomponent systems at the nano-, micro- and macro-levels (Arel and Aydin 2018, Aydin and Arel 2017, Bogdanov and Ibragimov 2017).

One of the main properties of protective structures is impact strength. There are a number of technological ways to increase it. One of them is to increase the static strength of concrete by optimizing the formulation and manufacturing technology (Lesovik *et al.* 2014). Another direction is to introduce a low-hard porous dispersed damping additives into the concrete mix (Mosaberpanah and Eren 2017a, Zagorodnjuk *et al*. 2016). However, such concretes provide a relatively small increase in impact strength, which is not sufficient for defensive structures under the conditions of the action of modern definitions of destruction by creating the large shock loads on the building envelope. The use of fiber-reinforced concrete with enhanced dynamic strength in the production of structures for protective structures is promising. Dispersed reinforcement allows to significantly increase the entire set of mechanical properties of concrete (Lesovik *et al*. 2014, Volodchenko *et al*. 2015).

In previous studies, the theoretical foundations of the creation of composite binders (CB) were developed using various pozzolanic additives as well as silica-containing components, in addition to concrete-based concrete, natural and man-made aggregates, along with dispersed reinforcement [14, 18, 19]. However, the question of using new types of ultra-fine mineral additives, with considerations to the principles of their compatibility to ensure the required performance characteristics of CB by reducing the cement consumption and replacing with ultra-fine RHA, LCW, and QS have not been studied; It is necessary to develop composites of a new generation, which are characterized by a special set of required high rates of physical and mechanical properties: static and dynamic compressive strength, tensile strength, elastic modulus. Thus, the article puts forward a working hypothesis about the possibility of creating self-compacting low-permeable fiber-reinforced concrete by using ultra-fine RHA, LCW, and QS and controlling the processes of structure formation as a result of the use of multicomponent composite cement and disperse reinforcement.

2. Materials and experimental methodology

Objective of paper: to develop effective self-compacting dispersion-reinforced concretes of quaternary multicomponent composite cement

To achieve this objective, the following tasks were undertaken:

- the study of the material composition, structure and quality characteristics of the source materials.
- substantiation of the possibility of using the multicomponent composite cement as a component of binding systems.
- development of binding compositions based on Portland cement and multicomponent composite cement additive; selection of the optimal composition and parameters of manufacturing the CB with regard to ensuring the required mechanical and rheological characteristics of self-compacting fiber-reinforced concrete;
- experimental determination of the mechanical properties of FRSCC including tensile strength, modulus of elasticity, number of blows for formation the first crack, and number of blow for destruction on FRSCC.

2.1 Materials

2.1.1 Composite binder

Considering the fact that Russia has one of the leading places in the world in rice harvesting (987,000 ton in 2018) the technology has been developed to produce a rice husk ash (RHA) as binder material, which involves the heat treatment of rice husks (from the farm located in southern of Russian Far East) in a muffle at a temperature of 800-900°C. The choice of this technology was to obtain both amorphous and crystalline phases of rice husk ash. Table 1 presents the chemical composition of rice husk and RHA powder (with almost 95% silica).

In addition to the RHA and Portland cement (OPC, ASTM C 150 type I), limestone crushing waste (LCW) and quartz sand were included in the composition of the composite binder. Table 2 enlists the chemical compositions of the OPC, LCW and quartz sand used. The particle size distribution for RHA and CEM I shows a high specific surface of the RHA (Fig. 1).

Table 1 The chemical composition of rice husk and RHA

Raw	CaO	SiO_2	Al_2O_3	Fe_2O_3	MgO	SO_3	Na_2O	K_2O	LOI
Rice husk	0.61	15.64	0.24	0.12	0.45	0.18	0.48	0.28	82.1
RHA	0.56	94.58	0.22	0.11	0.23	0.05	0.27	0.26	3.72

Table 2 The chemical composition of OPC, LCW and quartz sand

Raw	CaO	SiO_2	Al_2O_3	Fe_2O_3	MgO	SO_3	Na_2O	K_2O	TiO_2	LOI
OPC	68.2	20.9	6.00	3.51	1.41	2.32	0.21	0.64	-	1.54
LCW	44.2	7.49	3.33	0.24	2.57	-	-	-	0.24	38.7
Quartz sand	0.01	99.4	0.25	0.12	-	-	-	0.03	0.07	-

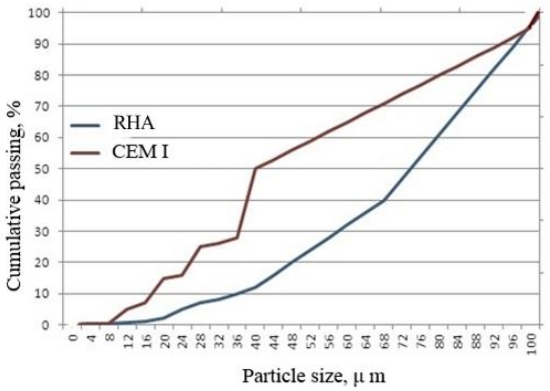

Fig. 1 Particle size distribution for RHA and CEM I

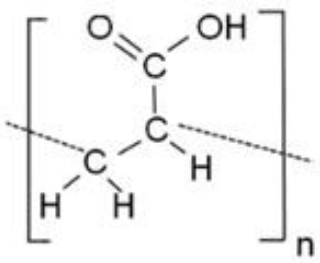

Fig. 2 Molecular model of superplasticizer Pantarhit PC 160

Table 3 Specifications of used types of fibers

Characteristics	Steel fiber	Basalt fiber
Manufacturer	Universum, Russia	Akstrimpromservis, Russia
Tensile strength, MPa	600-1500	3500
Fiber diameter, mm	1.2	13 ·10-3
Fiber length, mm	13	6±1,5
Elastic modulus, GPa	190	75
Elongation ratio, %	3.5	3.2
Melting temperature, °C	1550	1450
Alkali and corrosion resistance	middle	high
Density, kg/m^3	7800	2600

The study on the milling of the composite binder was carried out by vario-planetary mill Pulverisette-4 (Germany). The milling was carried out for 170 minutes with the implementation of control measurements of the specific surface area of the comminuted material for every 10 minutes.

2.1.2 Superplasticizer

Pantarhit PC 160 was used as a superplasticizer, which was a light gray powder with a bulk density of 450 m^3/kg and a molecular weight of 11,600 g/mol. The superplasticizer active ingredient was polyacrylic acid with the chloride content of less than 0.1%, and the pH of a 20% solution under normal conditions was 6.5±1. The Molecular model is given in Fig. 2.

2.1.3 Fiber

Two types (steel brass-plated and basalt) of fiber were used as disperse reinforcement at ratio of 1% to 2% by weight of mix. Specifications of used types of fibers are listed in Table 3.

2.1.4 Aggregate

In this study, Quartz sand from the Razdolnensky deposit (Russia) was used as fine aggregate. Grain composition and physico-mechanical properties of sand are given in Table 4 and Table 5.

2.2 Experimental methodology

This study has been carried out into two steps; in the first step, the composition of the composite binder based on CEM I 42.5N (58-70%), husk ash (25-37%), quartz sand (2.5-7.5%) and limestone crushing waste (2.5-7.5%) were optimized. In the second step, two types (steel brass-plated and basalt) of fiber were used to the optimized SCC with the optimum CB as dispersing reinforcement at a ratio of 1% to 2% by weight of the mix.

Table 4 Grain composition of used sand

The content of coarse-grained impurities, %		Remains on the sieves, %	Particle size distribution Sieve sizes, mm						Fineness modulus
>10 mm	>5 mm		2.5	1.25	0.63	0.315	0.16	<0.15	
-	-	partial	2.0	6.5	34.5	41.5	13.0	2.5	2.4
		full	2.0	8.5	43.0	84.5	97.5	100	

Table 5 Physico-mechanical properties of used sand

Bulk density, kg/m^3	True density, kg/m3	Void volume, %	Content of clay and dust particles, %
1343	2630	48.9	0.5

Table 6 Mix design for the selection of the optimal composition of CB

Sample Coding	Quaternary Composition of CB, %				SP, % of CB	*w/b*	Viscosity, %
	CEM I	QS	LCW	RHA			
CEM I	100	-	-	-	-	0.25	25.9
CB1-1	61	3.5	3.5	32	1.0	0.25	22.3
CB1-2	62	3.5	3.5	31	1.3	0.25	21.6
CB1-3	63	3.5	3.5	30	1.6	0.25	20.3
CB2-1	57.5	5.25	5.25	32	1.0	0.25	22.7
CB2-2	58.5	5.25	5.25	31	1.3	0.25	21.5
CB2-3	59.5	5.25	5.25	30	1.6	0.25	20.8
CB3-1	54	7	7	32	1.0	0.25	23.0
CB3-2	55	7	7	31	1.3	0.25	22.1
CB3-3	56	7	7	30	1.6	0.25	22.6

Note: QS – quartz sand; LCW – limestone crushed waste; RHA – rice husk ash; SP – superplasticizer.

2.2.1 Phase one; Determination of optimum composition of CB

In this study, based on the literature review, a wide range of CB compositions were designed to find the optimum characteristic of CB. The various ratios for different CB composition are given in Table 6.

2.2.1.1 Mixing procedure

The first phase of study was aimed at optimizing the composition of the composite binder based on CEM I 42.5N (58-70%), active silica-containing dditive (25-37%), quartz sand (2.5-7.5%) and limestone crushing waste (2.5-7.5%). At the same time, an important clarification was made which specifying that the superplasticizer (1.0-1.6% by weight of the CB mixture) was not part of the composite binder and not subjected to joint grinding, but in a certain way affected the binding properties of the obtained composite. The use of superplasticizer allowed for the provision of a water-binder ratio of 0.25. The composite pastes were obtained using a mixer (Technotest, France) for

1 min at low speed (60 rpm) and 4 min at high speed (120 rpm). The fresh mixes were maintained in molds for 24 h after casting; then they were removed and kept to cure in air for 28 days.

2.2.1.2 Flowability of CB

The viscosity (normal density) of the mixtures was studied on the RheoStress 600 rotational viscometer (Haake Technik GmbH). The consistency of the CB paste was taken as the normal density, in which the pestle does not reach 5-7 mm to the bottom of the measuring container. The study of the rheological parameters of the mixtures using a viscometer was carried out 5 minutes after mixing. To ensure the reliability of the research results and the possibility of their comparison, the compositions of the mixtures were molded with the same procedure.

2.2.2 Phase two; Effect of fiber on FRSCC

After finding the optimum CB, in phase II, two types of fiber (steel brass-plated and basalt) were used to the optimized SCC with the optimum CB as disperse reinforcement at 6 different ratios of 1% to 2% by weight of mix for each type.

2.2.2.1 Mixing procedure

Mortars were mixed in a mixer for at least 5min. Cement, filler, sand and half of the water were first mixed. Then, the remaining water, superplasticizer and fibers were added slowly to ensure full dispersion. After that, the fresh mortar was casted in various moulds: 100×100×100 mm cubic (for compressive strength test), 70×70×70 mm cubic (for elastic modulus test), prisms with an edge length of 100×100×500 mm (for tensile strength test) and panel dimensions 600×600×50 mm (for first crack strength test). The specimens were vibrated on the standard vibrating machine for two minutes. After twenty-four hours, specimens were taken off the moulds and immersed in air at a temperature of 20±2°C for 28 days, i.e., until the day of testing.

2.2.2.2 Flowability of FRSCC

At the first stage, immediately after mixing in a mixer, all test specimens were tested for spreading of cone according to ASTM C 1611/C 1611M-05 (in millimeters) and the measure of speed, i.e., that time (in seconds) that was needed to spread the mixture cone to a diameter of 500 mm.

At the next stage, the mixtures were subjected to the following tests. The time of passing the mixture through the *V*-funnel was determined in accordance to EN 12350-9. This test gives adequate results, because the maximum size of the aggregate does not exceed 20 mm. The device consists of a *V*-frame with a capacity of 10 liters of stainless steel with waterproof sliding inner surfaces. The top edge is smooth and reinforced, and the outlet is equipped with a sealing valve.

Determination of the flow rate of the mixture was made in the *L*-box in accordance to EN 12350-10. The test box consists of a concrete mix tank with sliding internal surfaces, three obstacles and a test basin.

The study of the behavior of the mixture in the *U*-box is used to measure the ability to push concrete accordance to EFNARC 2002. The apparatus consists of a vessel, which is divided in the middle by a wall into two compartments; between the two sections there is a hole with a sliding gate. Reinforcing rods with a nominal diameter of 13.4 mm are mounted on the gate with a distance from the center to the center of 50 mm. This creates a distance between the rods of 35 mm. The left section is filled with about 20 liters of concrete, then the gate rises and the concrete flows upwards to another section. Concrete height in both sections were measured.

The study of the segregation of self-compacting concrete mixture was carried out using Static Segregation Column Mold-HC-3666 with accordance to EFNARC 2002. Used to determine the potential for static delamination of self-compacting concrete by measuring the content of fiber and aggregate in the upper and lower parts of a cylindrical column. During the tests, the concrete mixture is poured into the top of the column and held for 15 minutes. Then the aggregate and the fiber from the upper and lower parts of the column are collected, washed from the cement paste and sieved through a 4.75 mm sieve. The segregation index (SI) is then calculated by comparing the masses in the upper and lower parts as formula (1)

$$SI = \frac{M_l - \mathrm{M}_u}{M_l + \mathrm{M}_u} \quad (1)$$

2.2.2.3 Tensile strength test of FRSCC

Tensile splitting strength of the prisms with an edge length of 100×100×500 mm specimens was tested according to EN 12390-6 (2009).

2.2.2.4 Elastic modulus of FRSCC

The values of the modulus of elasticity were determined for samples at 30% of the failure load as Formula (2).

$$\mathrm{E}_\sigma = \frac{\sigma_1}{\varepsilon_{1y}} \quad (2)$$

here σ_1- is equal to the voltage increment from the conditional zero to 30% of the destructive external load; ε_{1y}- is equal to the increment of the elastic instantaneous relative longitudinal deformation of the sample, corresponding to the same level of load (measured at the beginning of each stage of its application).

2.2.2.5 First crack strength of FRSCC

The crack width of the entire fiber-reinforced concrete panel dimensions 600x600x50 mm was measured using a Dino-Lite AM3713TB microscope (AnMo Electronics Corporation, Taiwan) immediately after the appearance of the first crack; later the propagation of cracks in the panel was studied. The ratio of the number of shocks causing failure, N_f to the number of shocks causing the first crack, N_c is defined as the coefficient of impact strength $\mu_i = N_f/N_c$.

2.2.2.6 Destruction test of FRSCC

There were 2 series of tests: on the panels and on the cylinders. The panels of 600×600×50 mm were removed from the mold 24 hours after casting and left in the laboratory until the testing age. The impact ability of the

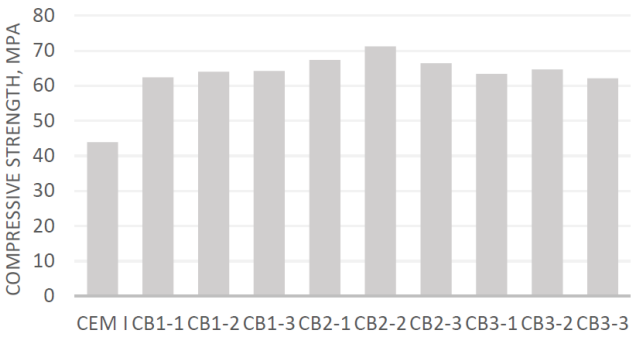

Fig. 3 Effect of different compressive strength on different CB

panels was tested on the 28th day. The impact strength test was carried out with the help of a falling drummer on the basis of the international regulatory document ACI Committee 544; the impact-resistant specimen was subjected to repeated strikes in one place. In this test, a hammer weighing 10 kg fell from a height of 600 mm on the panel. Impact energy E_i was calculated by the formula (3).

$$E_i = m \cdot g \cdot h \cdot N \quad (3)$$

ɔdе m- hummer weight=10 kg; *g*=9,81 m/s2; *N*–number of blows.

The study of the cylinders was carried out on the same device. In the study of single blows, three different drop heights of the hummer were considered, that is, 40 cm, 60 cm and 80 cm.

3. Experimental results and discussion

3.1 Phase one; Designed CB

The optimization of the composition of the composite binder based on CEM I 42.5N (58-70%), active silica-containing additive (25-37%), quartz sand (2.5-7.5%) and limestone crushing waste (2.5-7.5%) in order to develop the SCC by measuring the of compressive strength were carried out.

3.1.1 Compressive strength

Effect of different compressive strength on different CB proportion is given in Fig. 3. It is clearly observed that the CB2-2 containing 58.5% cement reached a maximum compressive strength of 71.21 MPa which improved the compressive strength by 62.25% compared to the control concrete mix (CEM I) as adding RHA as SCMs shows the ability of binder to improve the compressive strength by reducing large number of pores and increasing the pozzolanic activity because of its physical and chemical properties. Therefore, the presence of RHA makes the microstructure of binder more dense and homogeneous (Arel and Aydin 2018, Mosaberpanah 2019). It should be noted the savings of the clinker component in the amount of more than 40% gives a tangible economic and environmental effects (Peshkova *et al.* 2016).

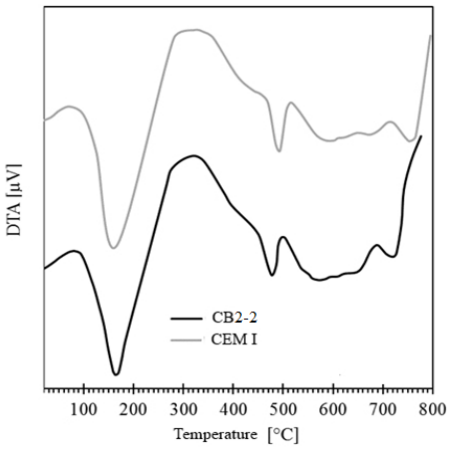

Fig. 4 DTA results for pure cement and cement of CB2-2

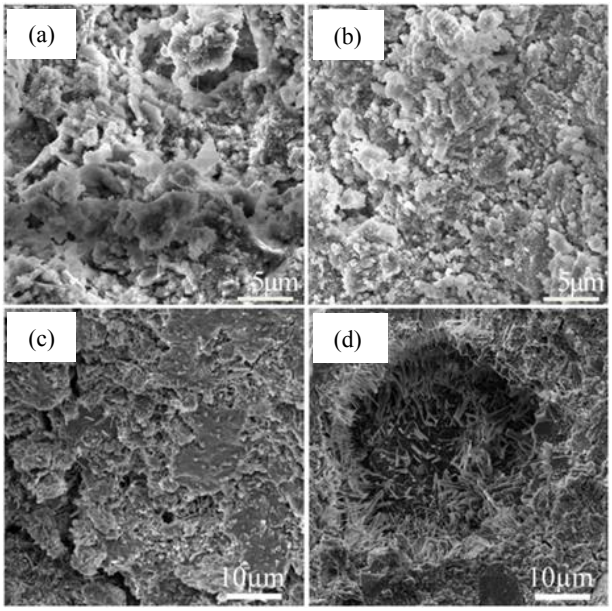

Fig. 5 Microstructure of neoplasms (age 28 days): pure cement (a), (c) and cement on the developed CB2-2 (b), (d)

3.1.2 Differential thermal analysis

This was observed by comparing the differential thermal analysis results of the additive-free cement and cement-composite of the CB2-2 (Fig. 4) As decreasing the area of the "endothermic effect" of the cement available in CB2-2 at the temperature of about 160ºC shows a decrease in the content of gel including neoplasms due to their transition to a crystalline state. On the other hand, the growth of the peak area on the thermogram of the cement-free additive shows a greater content of Portlandite in its composition. the endothermic effect (475°C-corresponds to the dehydration of calcium hydroxide (Soragni 2017). The last endothermic effect (525-650°C) is probably associated with the dissociation of $CaCO_3$.

3.1.3 Microstructure analysis

The morphology of pure cement and cement on the developed CB2-2 are shown in Fig. 5. All tested were provided after 28 days compressive strength tests. Fig. 5(a) shows the irregular particles and also micropores which is

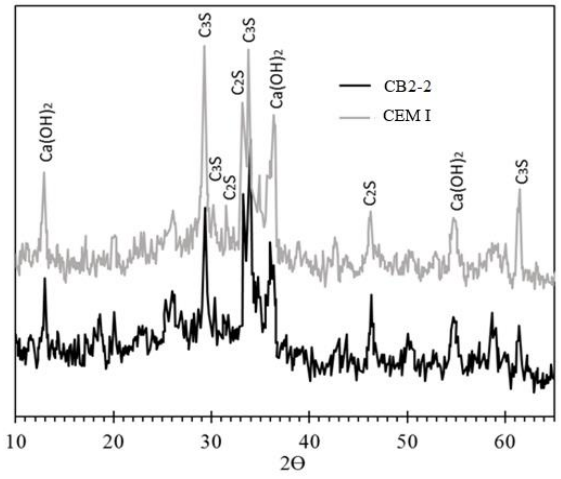

Fig. 6 XRD of neoplasms

also visible in Fig. 5(c) which may cause poor performance in durability and strength. In opposite, the cement-composite which has a structure with a reduced content of voids and microcracks (Fig. 5(b)) showes higher compressive strength than unblended cement. There are clearly visible systems of needle and lamellar species that fill isometric and anisometric pores (Fig. 5(d)) which leads to the formation of a rigid matrix with reduced porosity, and, accordingly, to the hardening of the cement-composite.

This is also confirmed by the composition of the neoplasms: for CB2-2 (Fig. 6), a reduced intensity of peaks corresponding to clinker minerals is noted: alite with *d/n*=3.04; 2.97; 2.78; 2.74; 2.75; 2.61; 2.18; 1.77 Å and belite with *d/n*=2.89; 2.67; 2.72; 2.76; 2.75; 2.78; 1.77 Å, which indicates the intensification of hydration processes using CB. In addition, CB contributes to reduce the intensity of the peaks of Portlandite with *d/n*=4.93; 2.63; 1.93 Å.

Thus, theoretical concepts of CB2-2 synthesis have been developed, consisting in optimizing the processes of structure formation through the use of a multicomponent composite cement, together with Portland cement, milled in a vario-planetary mill with a specific surface of 550 m^2/kg. The amorphous silica in the modifier composition intensifies the binding of calcium hydroxide formed during the hydration of C3S which helps to reduce the basicity of the cement-composite, while reducing the growth of portlandite crystals. On the other hand, contributing to the crystallization of low-base low-soluble CSH, compacting the microstructure of the cement-composite. Limestone particles contribute to the formation of calcium hydrocarbonate and, together with fine ground quartz sand, act as a microfiller, clogging the pores of the cement (Ergenç *et al.* 2018).

3.2 Phase II; Effect of fiber on FRSCC

In phase II and after finding the optimum CB, two types of fibers, steel brass-plated and basalt, were used to the optimized SCC with the optimum CB as disperse reinforcement at 6 different ratios of 1% to 2% by weight of mix for each type.

3.2.1 Fresh properties of FRSCC

For the flowability of FRSCC, the fibrous-concrete mixes were designed on the basis of achieving the cone spreading of an average diameter of 680 ± 30 mm, which was achieved as a result of a change in the water-binder ratio. These values of the cone flare correspond to the SF2 grade (according to EFNARC 2002) of the self-compacting concrete mix. The results of the flowability tests for SCC are shown in Fig. 7.

In the context of these studies (Huang *et al.* 2017, Le *et al.* 2015, Mosaberpanah 2019), attention was focused on the fact that the increase in the amount of RHA in the binder leads to a decrease in the workability of the mixture as a result of a large active area of ash particles, which, respectively, entails an increased water demand necessary for the particles to slip along each other. In opposite, there are several studies mentioning, adding RHA increases the flowability of SCC (Arel and Aydin 2018, EFNARC 2002, Safiuddin *et al.* 2012, Sua-iam and Makul 2014). The pore size distribution of RHA is the key of aforementioned contradiction which control the flowability of mortars. Fig. 7 shows cement-composite including RHA increasing the flowability of CB compared to pure cement as it is reported finer pore size distribution of RHA reduces water absorption as if the dosage of superplasticizer is increased. It could be concluded that, the finer particle sizes have more advantage in enhancing appropriate workability and pozzolanic activity (Bui *et al.* 2005).

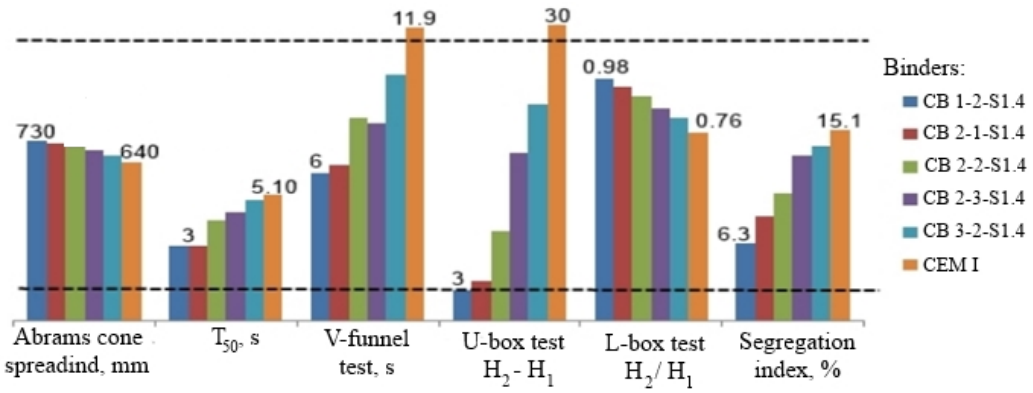

Fig. 7 The results of the flowability tests

Table 8 Effect of different fiber types and percentage on Mechanical properties of FRSCC

Samples	Tensile Strength, MPa	Modulus of Elasticity, Gpa	Number of blows for formation the first crack	Number of blow for destruction
CB2-2	15.2	39.25	10	50
CB2-2-S1.0	15.7	42.00	35	300
CB2-2-S1.2	15.8	42.25	65	600
CB2-2-S1.4	16.2	43.50	89	850
CB2-2-S1.6	16.4	43.25	86	850
CB2-2-S1.8	16.0	42.75	49	450
CB2-2-S2.0	15.7	42.00	18	110
CB2-2-B1.0	15.6	40.85	30	250
CB2-2-B1.2	15.5	41.60	61	570
CB2-2-B1.4	15.8	42.80	93	790
CB2-2-B1.6	15.7	42.90	85	800
CB2-2-B1.8	15.5	41.00	47	400
CB2-2-B2.0	15.5	40.85	22	80

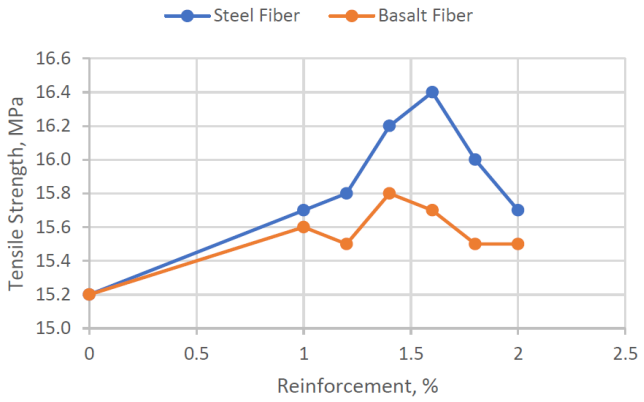

Fig. 8 The effect of the percentage of reinforcement by various types of fibers on tensile strength

3.2.2 Mechanical properties of FRSCC

Different mechanical tests such as tensile strength, modulus of elasticity, number of blows for formation the first crack, and number of blow for destruction on FRSCC carried out which are summarized in Table 8. It revealed that the use of basalt fiber instead of steel fiber has led to some decrease in the mechanical properties of concrete.

Fig. 8 shows the effect of different percentage of steel and basalt fibers on tensile strength of FRSCC. It is explicitly understandable that steel fiber increases more the tensile strength of FRSCC than basalt fiber. It is found that the steel fiber improves the tensile strength of FRCC at the optimum point of 1.6% (CB2-2-S1.6) for 7.9%; however, the basalt fiber improved at the optimum point of 1.4% (CB2-2-B1.4) for 3.9% compared to the control mix.

The effect of different types and percent of fibers on modulus elasticity of FRSCC are given in Fig. 9. It is derived that steel fiber performed better than basalt fiber on modulus elasticity of FRSCC as 1.4% of steel fiber by weight of mix improved the modulus of elasticity for 10.8%; however, 1.6% of basalt fiber by weight of mix increased for 9.3% compared SCC.

It was observed that there are optimal dosages of the fiber reinforcement for tensile strength and modulus of

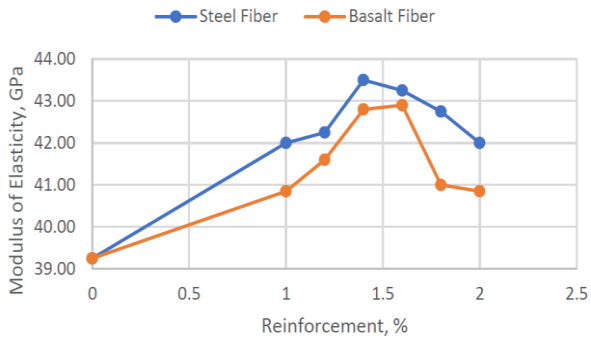

Fig. 9 The effect of the percentage of reinforcement by various types of fibers on elastic modulus of fiber-reinforced concrete

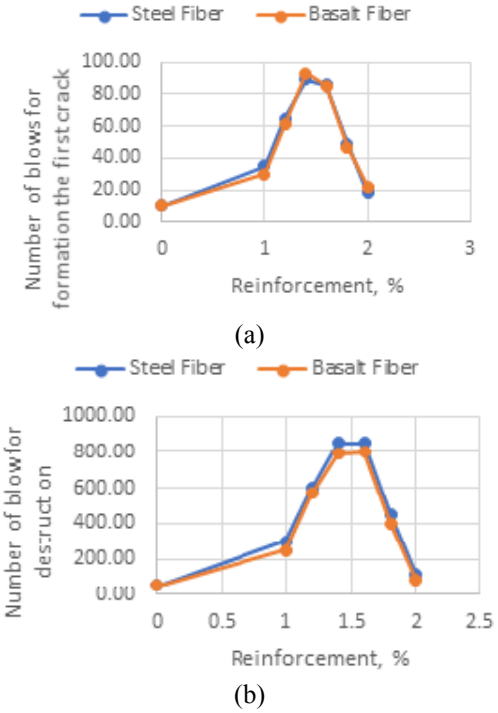

Fig. 10 Number of blows for first crack strength (a) Number of blows for Destruction (b)

elasticity as after the optimum reinforcement dosage, the performance of FRSCC will be reduced. This situation would be explained as after the optimal dosage of fiber reinforcement, the fibers cannot be longer evenly distributed throughout the volume and they might accumulate in some places (Zak *et al.* 2016). Therefore, the strength of the composite is gradually decreasing after the optimum dosage of fiber.

The impact strength of FRSCC in terms of first crack strength (Fig. 10(a)) and destruction (Fig. 10(b)) by various types of fiber were carried out. It is found that after adding steel or basalt fiber, the strength of concrete (before the formation of the first crack) increases up to 9 times compared with the corresponding mixtures without fiber. Both steel and basalt fibers are effective in preventing the growth of microcracks and reducing the spread of these cracks (Wang *et al.* 2019) before the cracks merged to form macrocracks.

4. Conclusions

In this paper, two phase experiments were carried out on Development of Fiber Reinforced Self-Compacting Concrete (FRSCC). In phase one, a wide range of CB compositions including CEM I 42.5N (58-70%), Rice husk ash (25-37%), quartz sand (2.5-7.5%) and limestone crushing waste (2.5-7.5%) were applied to find the optimum characteristic of CB. The main observations are summarized below:

- The CB2-2 containing 58.5% cement reached a maximum compressive strength of 71.21 MPa which improved the compressive strength by 62.25% compared to the control concrete mix (CEM I).
- The savings of the clinker component in the amount of more than 40% gives a tangible economic and environmental effect.
- The optimum CB (CB2-2) shows a greater content of Portlandite in its composition than control mix.
- The amorphous silica in the optimum CB intensifies the binding of calcium hydroxide formed during the hydration of C3S, helps reduce the basicity of the cement-composite, while reducing the growth of portlandite crystals.

In Phase two, two types of fiber (steel brass-plated and basalt) were used to optimize SCC with the optimum CB as disperse reinforcement at 6 different ratios of 1% to 2% by weight of mix for each type. In This phase, below observations were found:

- The Steel fiber better performed than basalt fiber on tensile strength and modulus of elasticity of FRSCC;
- Steel and basalt fibers had almost the same performance on number of blows for first crack strength and Destruction.
- There is an optimum percentage of fiber addition between 1.4% and 1.6% by mix weight on different mechanical tests as after the optimal percentage, the fibers can no longer be evenly distributed throughout the volume and accumulates in some places.

Various studies have been made to produce cementitious binder by adding/replacing different additives to cement to obtain high rates of physical and mechanical properties. A combination of different mineral admixtures especially waste or by-product materials with cement increase strength and durability and modify the properties of cement and concrete. However, there are several gaps of study and more study is needed to mix these waste materials as the ternary and especially quaternary mixtures with different particle size distributions and proportions with cement.

References

Abdelgader, H., Najjar, M. and Azabi, T. (2010), "Study of underwater concrete using two-stage (preplaced aggregate) concrete in Libya", *Struct. Concrete*, **11**(3), 161-165.

AlTaan, S., Mohammed, A. and Al-Jaffal, A. (2012), "Breakout capacity of headed anchors in steel fibre normal and high strength concrete", *Asian J. Appl. Sci.*, **5**(7), 485-496. https://doi.org/10.3923/ajaps.2012.485.496.

Arel, H.Ş. and Aydin, E. (2018), "Use of industrial and agricultural wastes in construction concrete", *ACI Mater. J.*, **115**(1), 55-64.

Aydin, E. and Arel, H.Ş. (2017), "Characterization of high-volume fly-ash cement pastes for sustainable construction applications", *Constr. Build. Mater.*, **157**, 96-107. https://doi.org/10.1016/j.conbuildmat.2017.09.089.

Bogdanov, R. and Ibragimov, R. (2017), "Process of hydration and structure formation of the modified self-compacting concrete", *Mag. Civil Eng.*, **73**(5), 14-24.

Bui, D., Hu, J. and Stroeven, P. (2005), "Particle size effect on the strength of rice husk ash blended gap-graded Portland cement concrete", *Cement Concrete Compos.*, **27**(3), 357-366. https://doi.org/10.1016/j.cemconcomp.2004.05.002.

Chen, Y., Cen, G. and Cui, Y. (2018), "Comparative study on the effect of synthetic fiber on the preparation and durability of airport pavement concrete", *Constr. Build. Mater.*, **184**, 34-44. https://doi.org/10.1016/j.conbuildmat.2018.06.223.

Danish, A. and Mosaberpanah, M.A. (2020), "Formation mechanism and applications of cenospheres: a review", *J. Mater. Sci.*, **55**, 1-19. https://doi.org/10.1007/s10853-019-04341-7.

Dauji, S. and Bhargava, K. (2016), "Estimation of concrete characteristic strength from limited data by bootstrap", *J. Asian Concrete Fed.*, **2**(1), 81-94. http://dx.doi.org/10.18702/acf.2016.06.2.1.81

Djelloul, O.K., Menadi, B., Wardeh, G. and Kenai, S. (2018), "Performance of self-compacting concrete made with coarse and fine recycled concrete aggregates and ground granulated blast-furnace slag", *Adv. Concrete Constr.*, **6**(2), 103-121. https://doi.org/10.12989/acc.2018.6.2.103.

EFNARC, S. (2002), Guidelines for Self-Compacting Concrete, Association House, London, UK.

Ergenç, D., Gómez-Villalba, L.S. and Fort, R. (2018), "Crystal development during carbonation of lime-based mortars in different environmental conditions", *Mater. Characteriz.*, **142**, 276-288. https://doi.org/10.1016/j.matchar.2018.05.043.

Fediuk, R., Lesovik, V., Mochalov, A., Otsokov, K., Lashina, I. and Timokhin, R. (2018), "Composite binders for concrete of protective structures", *Mag. Civil Eng.*, **82**(6), 208-218. https://doi.org/10.18720/MCE.82.19.

Huang, H., Gao, X., Wang, H. and Ye, H. (2017), "Influence of rice husk ash on strength and permeability of ultra-high performance concrete", *Constr. Build. Mater.*, **149**, 621-628. https://doi.org/10.1016/j.conbuildmat.2017.05.155.

Khaloo, A., Raisi, E.M., Hosseini, P. and Tahsiri, H. (2014), "Mechanical performance of self-compacting concrete reinforced with steel fibers", *Constr. Build. Mater.*, **51**, 179-186. https://doi.org/10.1016/j.conbuildmat.2013.10.054.

Le, H.T., Kraus, M., Siewert, K. and Ludwig, H.M. (2015), "Effect of macro-mesoporous rice husk ash on rheological properties of mortar formulated from self-compacting high performance concrete", *Constr. Build. Mater.*, **80**, 225-235. https://doi.org/10.1016/j.conbuildmat.2015.01.079.

Lesovik, V., Alfimova, N. and Trunov, P. (2014), "Reduction of energy consumption in manufacturing the fine ground cement", *Res. J. Appl. Sci.*, **9**(11), 745-748. https://doi.org/10.3923/rjasci.2014.745.748.

Mosaberpanah, M.A. (2019), "Utilizing rice husk ash as supplement to cementitious materials on performance of ultra high performance concrete-A review", *Mater. Today Sustain.*, **7-8**, 100030. https://doi.org/10.1016/j.mtsust.2019.100030.

Mosaberpanah, M.A. and Eren, O. (2016), "Relationship between 28-days compressive strength and compression toughness factor of ultra high performance concrete using design of experiments", *Procedia Eng.*, **145**, 1565-1571. https://doi.org/10.1016/j.proeng.2016.04.197.

Mosaberpanah, M.A. and Eren, O. (2017a), "Effect of quartz

powder, quartz sand and water curing regimes on mechanical properties of UHPC using response surface modelling", *Adv. Concrete Concstr.*, **5**(5), 481-492. https://doi.org/10.12989/acc.2017.5.5.481.

Mosaberpanah, M.A. and Eren, O. (2017b), "Statistical models for mechanical properties of UHPC using response surface methodology", *Comput. Concrete*, **19**(6), 667-675. https://doi.org/10.12989/cac.2017.19.6.673.

Mosaberpanah, M.A. and Eren, O. (2018), "CO_2-full factorial optimization of an ultra-high performance concrete mix design", *Eur. J. Environ. Civil Eng.*, **22**(4), 450-463. https://doi.org/10.1080/19648189.2016.1210030.

Peshkova, G., Cherepovitsyn, A. and Tcvetkov, P. (2016), "Prospects of the environmental technologies implementation in the cement industry in Russia", *J. Ecolog. Eng.*, **17**(4), 17-24. https://doi.org/10.12911/22998993/64607.

Safiuddin, M., West, J. and Soudki, K. (2012), "Properties of freshly mixed self-consolidating concretes incorporating rice husk ash as a supplementary cementing material", *Constr. Build. Mater.*, **30**, 833-842. https://doi.org/10.1016/j.conbuildmat.2011.12.066.

Soragni, E. (2017), *Innovative Geopolymers Based on Metakaolin: Synthesis and Applications*. https://doi.org/10.6092/unibo/amsdottorato/7856.

Sua-iam, G. and Makul, N. (2014), "Utilization of high volumes of unprocessed lignite-coal fly ash and rice husk ash in self-consolidating concrete", *J. Clean. Prod.*, **78**, 184-194. https://doi.org/10.1016/j.jclepro.2014.04.060.

Suleymanova, L.A., Lesovik, V.S., Kara, K.A., Malyukova, M.V. and Suleymanov, K.A. (2014), "Energy-efficient concretes for green construction", *Res. J. Appl. Sci.*, **9**(12), 1087-1090.

Svintsov, A.P. and Shambina, S.L. (2018), "Influence of viscosity of vegetable and mineral oil on deformation properties of concrete and cement-sand mortar", *Constr. Build. Mater.*, **190**, 964-974. https://doi.org/10.1016/j.conbuildmat.2018.09.103.

Vincler, J.P., Sanchez, T., Turgeon, V., Conciatori, D. and Sorelli, L. (2019), "A modified accelerated chloride migration tests for UHPC and UHPFRC with PVA and steel fibers", *Cement Concrete Res.*, **117**, 38-44. https://doi.org/10.1016/j.cemconres.2018.12.006.

Volodchenko, A., Lesovik, V., Zagorodnjuk, L., Volodchenko, A. and Prasolova, E. (2015), "Influence of the inorganic modifier structure on structural composite properties", *Int. J. Appl. Eng. Res.*, **10**(19), 40617.

Wang, Q., Yi, Y., Ma, G. and Luo, H. (2019), "Hybrid effects of steel fibers, basalt fibers and calcium sulfate on mechanical performance of PVA-ECC containing high-volume fly ash", *Cement Concrete Compos.*, **97**, 357-368. https://doi.org/10.1016/j.cemconcomp.2019.01.009.

Yu, K.Q., Yu, J.T., Dai, J.G., Lu, Z.D. and Shah, S.P. (2018), "Development of ultra-high performance engineered cementitious composites using polyethylene (PE) fibers", *Constr. Build. Mater.*, **158**, 217-227. https://doi.org/10.1016/j.conbuildmat.2017.10.040.

Zagorodnjuk, L., Lesovik, V., Volodchenko, A. and Yerofeyev, V. (2016), "Optimization of mixing process for heat-insulating mixtures in a spiral blade mixer", *Int. J. Pharm. Technol.*, **8**(3), 15146-15155.

Zak, P., Ashour, T., Korjenic, A., Korjenic, S. and Wu, W. (2016), "The influence of natural reinforcement fibers, gypsum and cement on compressive strength of earth bricks materials", *Constr. Build. Mater.*, **106**, 179-188. https://doi.org/10.1016/j.conbuildmat.2015.12.031.